Inorg. Chem. **2008**, *47*, 4945−4951

Inorganic Chemistry
Article

Further Examples of the Failure of Surrogates to Properly Model the Structural and Hydrothermal Chemistry of Transuranium Elements: Insights Provided by Uranium and Neptunium Diphosphonates

Anna-Gay D. Nelson,[†] Travis H. Bray,[†] Wei Zhan,[†] Richard G. Haire,[‡] Todd S. Sayler,[†] and Thomas E. Albrecht-Schmitt*,[†]

Department of Chemistry and Biochemistry and Center for Actinide Science, Auburn University, Auburn, Alabama 36849, and Chemical Sciences Division, Oak Ridge National Laboratory, Oak Ridge, Tennessee 37831

Received February 12, 2008

In situ hydrothermal reduction of Np(VI) to Np(IV) in the presence of methylenediphosphonic acid (**C1P2**) results in the crystallization of $Np[CH_2(PO_3)_2](H_2O)_2$ (**NpC1P2−1**). Similar reactions have been explored with U(VI) resulting in the isolation of the U(IV) diphosphonate $U[CH_2(PO_3)_2](H_2O)$ (**UC1P2−1**), and the two U(VI) diphosphonates $(UO_2)_2[CH_2(PO_3)_2](H_2O)_3 \cdot H_2O$ (**UC1P2−2**) and $UO_2[CH_2(PO_3H)_2](H_2O)$ (**UC1P2−3**). Single crystal diffraction studies of **NpC1P2−1** reveal that it consists of eight-coordinate Np(IV) bound by diphosphonate anions and two coordinating water molecules to create a polar three-dimensional framework structure wherein the water molecules reside in channels. The structure of **UC1P2−1** is similar to that of **NpC1P2−1** in that it also adopts a three-dimensional structure. However, the U(IV) centers are seven-coordinate with only a single bound water molecule. **UC1P2−2** and **UC1P2−3** both contain U(VI). Nevertheless, their structures are quite distinct with **UC1P2−2** being composed of corrugated layers containing UO_6 and UO_7 units bridged by **C1P2**; whereas, **UC1P2−3** is found as a polar three-dimensional network structure containing only pentagonal bipyramidal U(VI). Fluorescence measurements on **UC1P2−2** and **UC1P2−3** exhibit emission from the uranyl moieties with classical vibronic fine-structure.

Introduction

The applications of diphosphonate ligands to nuclear waste remediation and actinide separation processes are well-developed.[1] As a general class of compounds, metal phosphonates have found relevance in many different areas including proton conductivity, ion-exchange, sensing, separations, and catalysis.[2] Over of the past five years the structural chemistry and physicochemical properties of metal diphosphonates have exploded into the literature.[3] Despite the importance of phosphonates and diphosphonates in actinide separation science, very little is known about the structural chemistry of crystalline solids of this type with elements beyond uranium.[4] Uranyl phosphonates represent an amazingly diverse group of compounds. The most significant discovery in this group is the uranyl phenylphosphonate system that undergoes a transformation from a cis (α-UPP) to trans (β-UPP) conformation at room temperature.[4c,d] Upon exposure to Na^+ or Ca^{2+} cations in an aqueous environment, both of these phases transform from linear chain structures into a hollow nanotubular form, γ-UPP.[4b]

We recently demonstrated that both Np(IV) and Np(VI) phosphonates can be prepared via controlled in situ hydrothermal redox processes that allow for slow kinetics of crystal growth.[5] This work provided the first examples of thoroughly characterized transuranium phosphonates. Herein we present another instance of the hydrothermal reduction of Np(VI) to Np(IV) that leads to the isolation of a Np(IV) diphosphonate. We also demonstrate that this type of chemistry is possible with uranium, and give examples of both U(IV) and

---

* To whom correspondence should be addressed. E-mail: albreth@auburn.edu.

[†] Auburn University.

[‡] Oak Ridge National Laboratory.

(1) (a) Nash, K. L. *J. Alloys Cmpd.* **1997**, *249*, 33. (b) Jensen, M. P.; Beitz, J. V.; Rogers, R. D.; Nash, K. L. *J. Chem. Soc., Dalton Trans.* **2000**, *18*, 3058. (c) Chiarizia, R.; Horwitz, E. P.; Alexandratos, S. D.; Gula, M. J. *Sep. Sci. Technol.* **1997**, *32*, 1.

(2) (a) Cao, G.; Hong, H.-G.; Mallouk, T. E. *Acc. Chem. Res.* **1992**, *25*, 420. (b) Clearfield, A. *Prog. Inorg. Chem.* **1998**, *47*, 371. (c) Clearfield, A. *Curr. Opin. Solid State Mater. Sci.* **2003**, *6*, 495. (d) Mao, J.-G. *Coord. Chem. Rev.* **2007**, *251*, 1493.

10.1021/ic800255h CCC: $40.75

U(VI) diphosponates. Finally, we address the long standing issue of whether lighter actinides like uranium can be used as surrogates for key transuranium elements like neptunium and plutonium.(6)

Experimental Section

Syntheses. UO_3 (98%, Strem), methylenediphosphonic acid, $CH_2(PO_3H_2)_2$ (**C1P2**, 98%, Alfa Aesar), were used as received. X-ray powder diffraction studies reveal that the UO_3 is actually a mixture of UO_3 and $UO_3 \cdot H_2O$. A 0.037 M stock solution of Np(VI) nitrate was prepare by first digesting NpO_2 in 8 M HNO_3 for 3 days at 200 °C (in an autoclave). The solution was reduced to a moist residue and redissolved in water. This solution was then ozonated for approximately 5 h to ensure complete oxidation of the neptunium to +6. UV−vis spectroscopy indicates that only Np(VI) is present. Reactions were run in PTFE-lined Parr 4749 autoclaves with a 23 mL internal volume for uranium, and with 10 mL internal volume autoclaves for neptunium. Distilled and Millipore filtered water was used in all reactions. Standard precautions were performed for handling radioactive materials during work with uranium. Semiquantitative EDX analyses were performed using a JEOL 7000F field emission SEM and confirmed the presence of the U and P in **UC1P2−1**, **−2**, and **−3**.

Caution! *^{237}Np ($t_{1/2} = 2.14 \times 10^6$ y) represents a serious health risk owing to its α and γ emission, and especially because of its decay to the short-lived isotope ^{233}Pa ($t_{1/2} = 27.0$ d), which is a potent β and γ emitter.*

All studies were conducted in a laboratory dedicated to studies on transuranium elements. This laboratory is located in a nuclear science facility and is equipped with HEPA filtered hoods and gloveboxes that are ported directly into the hoods. A series of counters continually monitor radiation levels in the laboratory. The laboratory is licensed by the state of Alabama (an NRC compliant state) and Auburn University's Radiation Safety Office. All experiments were carried out with approved safety operating procedures. All free-flowing solids are worked within the glovebox, and products are only examined when coated with either water or Krytox oil and water. There are some limitations in accurately determining yield with Np compounds because this requires weighing a dry solid, which poses certain risks as well as manipulation difficulties.

$Np[CH_2(PO_3)_2](H_2O)_2$ (NpC1P2−1). A 333 μL volume of a 0.037 M stock solution of Np(VI) was placed in an autoclave along with 12 mg of **C1P2**. The solution immediately changed from pink to green without the formation of a precipitate. The autoclave was sealed and heated at 180 °C for 3 days followed by slow cooling to room temperature over a 24 h period. The product consisted of dichroic pink/green prisms of **NpC1P2−1** and colorless mother liquor.

$U[CH_2(PO_3)_2](H_2O)$ (UC1P2−1), $(UO_2)_2[CH_2(PO_3)_2](H_2O)_3 \cdot H_2O$ (UC1P2−2), and $UO_2[CH_2(PO_3H)_2](H_2O)$ (UC1P2−3). UO_3 (207.5 mg, 0.725 mmol) was added to an autoclave along with 245.8 mg (1.40 mmol) of **C1P2**. Two milliliters of water was then added, and the autoclave was sealed. After heating for 3 days at 200 °C, the reaction mixture was cooled to room temperature by turning off the furnace. The product consisted of pale yellow tablets of **UC1P2−3** as the major product along with trace amounts of blue-green prisms of **UC1P2−1**. **UC1P2−2** can not be prepared rationally and requires the addition of $Nd(NO_3)_3$ to the reaction mixture. Although the Nd^{3+} is not incorporated into the final product, its presence is required for crystallization of **UC1P2−2**.

Crystallographic Studies. Single crystals of **$U[CH_2(PO_3)_2](H_2O)$ (UC1P2−1), $(UO_2)_2[CH_2(PO_3)_2](H_2O)_3 \cdot H_2O$ (UC1P2−2)**, and **$UO_2[CH_2(PO_3H)_2](H_2O)$ (UC1P2−3)** were mounted as normal on glass fibers. **$Np[CH_2(PO_3)_2](H_2O)_2$ (NpC1P2−1)** was glued with epoxy into a cryoloop to minimize chances of crystal loss during data collection while at the same time not compromising the data with uncorrectable absorption effects that would come with the use of nail-polish-painted capillaries that are often used with transuranics. The crystals were optically aligned on a Bruker APEX CCD X-ray diffractometer using a digital camera. Initial intensity measurements were performed using graphite monochromated Mo Kα ($\lambda = 0.71073$ Å) radiation from a sealed tube and monocapillary collimator. SMART (v 5.624) was used for preliminary determination of the cell constants and data collection control. The intensities of reflections of a sphere were collected by a combination of three sets of exposures (frames). Each set had a different ϕ angle for the crystal and each exposure covered a range of 0.3° in ω. A total of 1800 frames were collected with an exposure time per frame of 30 to 60 s, depending on the crystal.

---

(3) (a) Gomez-Alcantara, M. M.; Cabeza, A.; Olivera-Pastor, P.; Fernandez-Moreno, F.; Sobrados, I.; Sanz, J.; Morris, R. E.; Clearfield, A.; Aranda, M. A. G. *Dalton Trans.* **2007**, *23*, 2394. (b) Gomez-Alcantara, M. M.; Cabeza, A.; Moreno-Real, L.; Aranda, M. A. G.; Clearfield, A. *Microporous Mesoporous Mater.* **2006**, *88*, 293. (c) Sun, Z.-M.; Yang, B.-P.; Sun, Y.-Q.; Mao, J.-G.; Clearfield, A. *J. Solid State Chem.* **2003**, *176*, 62. (d) Sun, Z.-M.; Mao, J.-G.; Sun, Y.-Q.; Zeng, H.-Y.; Clearfield, A. *New J. Chem.* **2003**, *27*, 1326. (e) Mao, J.-G.; Wang, Z.; Clearfield, A. *J. Chem. Soc., Dalton Trans.* **2002**, *23*, 4457. (f) Arnold, D. I.; Ouyang, X.; Clearfield, A. *Chem. Mater.* **2002**, *14*, 2020. (g) Mao, J.-G.; Wang, Z.; Clearfield, A. *Inorg. Chem.* **2002**, *41*, 2334. (h) Poojary, D. M.; Vermeulen, L. A.; Vicenzi, E.; Clearfield, A.; Thompson, M. E. *Chem. Mater.* **1994**, *6*, 1845. (i) Mao, J.-G.; Wang, Z.; Clearfield, A. *Inorg. Chem.* **2002**, *41*, 2334. (j) Tang, S.-F.; Song, J.-L.; Li, X.-L.; Mao, J.-G. *Cryst. Growth Des.* **2007**, *7*, 360. (k) Tang, S.-F.; Song, J.-L.; Mao, J.-G. *Eur. J. Inorg. Chem.* **2006**, *10*, 2011. (l) Du, Z.-Y.; Ying, S.-M.; Mao, J.-G. *J. Mol. Struct.* **2006**, *788*, 218. (m) Ying, S.-M.; Mao, J.-G. *J. Mol. Struct.* **2006**, *783*, 13. (n) Sun, Z.-M.; Prosvirin, A. V.; Zhao, H.-H.; Mao, J.-G.; Dunbar, K. R. *J. Appl. Phys.* **2005**, *97*, 10B305/1–10B305/3. (o) Ying, S.-M.; Mao, J.-G. *J. Mol. Struct.* **2005**, *748*, 63. (p) Sun, Z.-M.; Mao, J.-G.; Dong, Z.-C. *Polyhedron* **2005**, *24*, 571. (q) Yang, B.-P.; Mao, J.-G. *Inorg. Chem.* **2005**, *44*, 566. (r) Yang, B.-P.; Sun, Z.-M.; Mao, J.-G. *Inorg. Chim. Acta* **2004**, *357*, 1583. (s) Song, J.-L.; Mao, J.-G.; Sun, Y.-Q.; Clearfield, A. *Eur. J. Inorg. Chem.* **2003**, *23*, 4218. (t) Ying, S.-M.; Mao, J.-G.; Yang, B.-P.; Sun, Z.-M. *Inorg. Chem. Commun.* **2003**, *6*, 1319–1322. (u) Liang, J.; Shimizu, G. K. H. *Inorg. Chem.* **2007**, *46*, 10449.

(4) (a) Dines, M. B.; DiGiacomo, P. M. *Inorg. Chem.* **1981**, *20*, 92. (b) Grohol, D.; Clearfield, A. *J. Am. Chem. Soc.* **1997**, *119*, 9301. (c) Grohol, D.; Clearfield, A. *J. Am. Chem. Soc.* **1997**, *119*, 4662. (d) Grohol, D.; Subramanian, M. A.; Poojary, D. M.; Clearfield, A. *Inorg. Chem.* **1996**, *35*, 5264. (e) Poojary, D. M.; Cabeza, A.; Aranda, M. A. G.; Bruque, S.; Clearfield, A. *Inorg. Chem.* **1996**, *35*, 5603. (f) Poojary, D. M.; Grohol, D.; Clearfield, A. *Angew. Chem., Int. Ed. Engl.* **1995**, *34*, 1508. (g) Poojary, D. M.; Grohol, D.; Clearfield, A. *J. Phys. Chem. Solids* **1995**, *56*, 1383. (h) Britel, A.; Wozniak, M.; Boivin, J. C.; Nowogrocki, G.; Thomas, D. *Acta Crystallogr.* **1986**, *C42*, 1502. (i) Grohol, D.; Clearfield, A. *Inorg. Chem.* **1999**, *38*, 751. (j) Doran, M. B.; Norquist, A. J.; O'Hare, D. *Chem. Mater.* **2003**, *15*, 1449. (k) Bao, S.-S.; Chen, G.-S.; Wang, Y.; Li, Y.-Z.; Zheng, L.-M.; Luo, Q.-H. *Inorg. Chem.* **2006**, *45*, 1124. (l) Cabeza, A.; Aranda, M. A. G.; Cantero, F. M.; Lozano, D.; Martínez-Lara, Bruque, S. *J. Solid State Chem.* **1996**, *121*, 181.

(5) Bray, T. H.; Nelson, A.-G. D.; Jin, G. B.; Haire, R. G.; Albrecht-Schmitt, T. E. *Inorg. Chem.* **2007**, *46*, 10959.

(6) (a) Runde, W.; Bean, A. C.; Albrecht-Schmitt, T. E.; Scott, B. L. *Chem. Commun.* **2003**, *4*, 478. (b) Bean, A. C.; Scott, B. L.; Albrecht-Schmitt, T. E.; Runde, W. *Inorg. Chem.* **2003**, *42*, 5632. (c) Weigel, F.; Engelhardt, L. W. H. *J. Less-Common Met.* **1983**, *91*, 339. (d) Bean, A. C.; Peper, S. M.; Albrecht-Schmitt, T. E. *Chem. Mater.* **2001**, *13*, 1266. (e) Gorden, A. E. V.; Shuh, D. K.; Tiedemann, B. E. F.; Wilson, R. E.; Xu, J.; Raymond, K. N. *Chemistry* **2005**, *11*, 2842. (f) Gorden, A. E. V.; Xu, J.; Raymond, K. N. *Chem. Rev.* **2003**, *103*, 4207. (g) Xu, J.; Radkov, E.; Ziegler, M.; Raymond, K. N. *Inorg. Chem.* **2000**, *39*, 4156.

Table 1. Crystallographic Data for $Np[CH_2(PO_3)_2](H_2O)_2$ (**NpC1P2-1**), $U[CH_2(PO_3)_2](H_2O)$ **(UC1P2-1)**, $(UO_2)_2[CH_2(PO_3)_2](H_2O)_3 \cdot H_2O$ (**UC1P2-2**), and $UO_2[CH_2(PO_3H)_2](H_2O)$ (**UC1P2-3**)

compound	NpC1P2−1	UC1P2−1	UC1P2−2	UC1P2−3
formula mass	441.02	426.00	776.03	458.00
color and habit	pink/green, prism	blue-green, prism	yellow, platelet	pale yellow, tablet
space group	$Pna2_1$ (No. 33)	*Pbca* (No. 61)	$P2_1/c$ (No. 14)	$Pna2_1$ (No. 33)
a (Å)	8.8418(15)	8.6227(6)	8.4574(5)	18.7589(12)
b (Å)	9.6381(16)	11.3457(7)	14.4419(8)	7.9134(5)
c (Å)	8.6627(15)	13.8635(9)	10.6003(6)	5.4368(4)
α (°)	90	90	90	90
β (°)	90	90	100.004(1)	90
γ (°)	90	90	90	90
V (Å^3)	738.2(2)	1356.27(15)	1275.05(13)	807.08(9)
Z	4	8	4	4
T (K)	193	193	193	193
λ (Å)	0.71073	0.71073	0.71073	0.71073
maximum 2θ (deg.)	28.35	28.30	28.32	28.32
ρ_{calcd} (g cm^{-3})	3.968	4.173	4.043	3.769
μ(Mo $K\alpha$) (cm^{-1})	145.18	243.96	256.89	205.31
$R(F)$ for $F_o^2 > 2\sigma(F_o^2)^a$	0.0149	0.0352	0.0278	0.0219
$R_w(F_o^2)^b$	0.0381	0.0825	0.0683	0.0569

[a] $R(F) = \sum||F_o| - |F_c||/\sum|F_o|$. [b] $R_w(F_o^2) = [\sum [w(F_o^2 - F_c^2)^2]/\sum wF_o^4]^{1/2}$.

For these compounds, determination of integrated intensities and global refinement were performed with the Bruker SAINT (v 6.02) software package using a narrow-frame integration algorithm. The data were treated with a semiempirical absorption correction by SADABS.[7] The program suite SHELXTL (v 6.12) was used for space group determination (XPREP), direct methods structure solution (XS), and least-squares refinement (XL).[8] The final refinements included anisotropic displacement parameters for all atoms and a correction for secondary extinction when necessary. Some crystallographic details are given in Table 1. Additional details can be found in the Supporting Information.

Fluorescence Spectroscopy. Fluorescence emission spectra of $(UO_2)_2[CH_2(PO_3)_2](H_2O)_3 \cdot H_2O$ (**UC1P2−2**) and $UO_2[CH_2(PO_3H)_2](H_2O)$ (**UC1P2−3**) were acquired using a PI Acton spectrometer (SpectraPro SP 2356, Acton, NJ) that is connected to the side port of an epi-fluorescence microscope (Nikon TE-2000U, Japan). The emission signal was recorded by a back-illuminated digital CCD camera (PI Acton PIXIS:400B, Acton, NJ) operated by a PC. For the compounds examined, the excitation was generated by a mercury lamp (X-Cite 120, EXFO, Ontario, Canada) filtered by a band-pass filter at 450−490 nm. The emission signal was filtered by a long-pass filter with a cutoff wavelength of 515 nm. The intensities of the spectra of the two compounds are not directly comparable to each other because different acquisition times and objective lenses were used.

Results and Discussion

Synthesis. The in situ hydrothermal reduction of Np(VI) to Np(IV) in the presence of methylenediphosphonic acid (**C1P2**) results in the crystallization of $Np[CH_2(PO_3)_2](H_2O)_2$ (**NpC1P2−1**) as the only product. Similar reactions have been explored with U(VI) resulting in much more complicated results. The major product of the reaction of UO_2^{2+} with **C1P2** is $UO_2[CH_2(PO_3H)_2](H_2O)$ (**UC1P2−3**). However, a small portion (ca. 5%) of the U(VI) is reduced to U(IV), producing $U[CH_2(PO_3)_2](H_2O)$ **(UC1P2−1)**. $(UO_2)_2[CH_2(PO_3)_2](H_2O)_3 \cdot H_2O$ (**UC1P2−2**) was produced serendipitously in separate studies designed to produce M^{n+}/UO_2^{2+}/**C1P2** compounds. However, the additional metals are not incorporated, and **UC1P2−2** crystallizes. We have been unable to make this compound without an additional metal present. Appropriate metals include Ln^{3+} (Ln = lanthanide) and Co^{2+}. There are subtle changes in the pH of the starting reactions mixtures used to produce **UC1P2−1** and **UC1P2−3** versus **UC1P2−2**. In the former case, the reactions are slightly less acidic (2.0) than those from which **UC1P2−2** are derived (1.4). The uranium reactions were repeated under identical conditions as those of **NpC1P2−1**. These reactions result only in the formation of **UC1P2−3**.

There are several curious features about the reaction of Np(VI) stock solutions with phosphonates that starts with the dramatic color change from pink to green that occurs upon addition of the phosphonate. UV−vis-NIR spectroscopic studies indicate that this color change corresponds to complexation of the NpO_2^{2+} cation by the phosphonate ligand and that no redox chemistry occurs. We were interested in gaining a deeper understanding of the in situ hydrothermal reduction of Np(VI) to Np(IV). These studies were initiated by simply subjecting 333 μL of the Np(VI) stock solution to the hydrothermal treatment already described in the *absence* of a phosphonate. Under these condition, the Np(VI) oxidizes water, and a mixture of Np(VI) and Np(V) is obtained (Rxn 1). The subsequent reduction of Np(V) to Np(IV) might occur via two different pathways. In Rxn 2, a precipitation-driven redox reaction is suggested, although we prefer Rxn 3, where the Np(IV) arises from disproportionation of Np(V) at low pH. The formation of a highly insoluble Np(IV) phosphonate would drive these reactions to completion in both cases.

$$4NpO_2^{2+} + 2H_2O \xrightarrow[H_2O]{180\ °C,\ 3\ d} 4NpO_2^{+} + 4H^{+} + O_2 \quad (1)$$

$$4NpO_2^{+} + 12H^{+} \xrightarrow[phosphonate]{180\ °C,\ 3\ d} 4Np^{4+}(phosphonate)_{(s)} + 6H_2O + O_2 \quad (2)$$

$$2NpO_2^{+} + 4H^{+} \xrightarrow[phosphonate]{180\ °C,\ 3\ d} Np^{4+}(phosphonate)_{(s)} + NpO_2^{2+} + 2H_2O \quad (3)$$

Comparison of the Structures of $Np[CH_2(PO_3)_2](H_2O)_2$ (NpC1P2−1) and $U[CH_2(PO_3)_2](H_2O)$ (UC1P2−1). NpC1P2−1 and **UC1P2−1** both adopt three-dimensional network structures where the An(IV) (An = U, Np) centers are

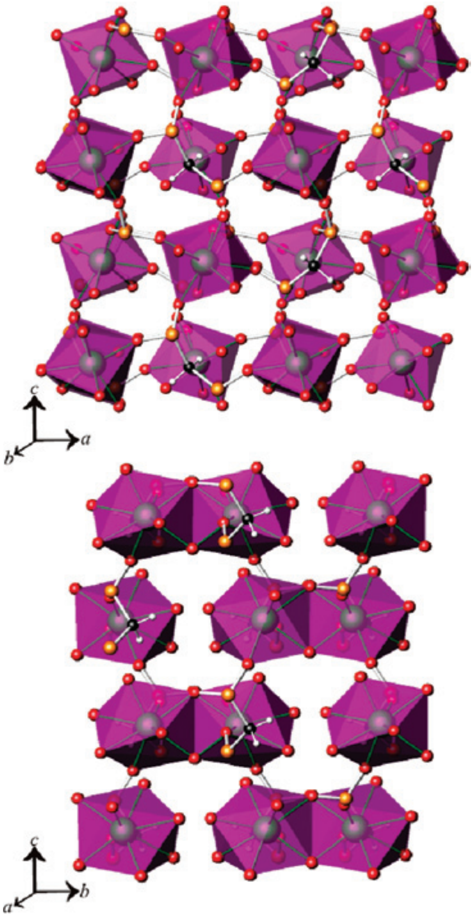

Figure 1. Two views of part of the structure of Np[$CH_2(PO_3)_2$](H_2O)$_2$ (**NpC1P2−1**) showing the polar three-dimensional framework constructed from Np(IV) centers that are bound by methylenediphosphonate and two water molecules to form isolated NpO_8 distorted dodecahedra. The bottom view shows the channels that the water molecules reside in. From this view it appears that the NpO_8 units share an edge, but this is an illusion. NpO_8 = orange, oxygen = red, phosphorus = orange, carbon = black, hydrogen = white. The majority of the methylenediphosphonate ligands have been omitted for clarity.

coordinated by methylenediphosphonate and water molecules. Various depictions of these structures are shown in Figures 1 and 2. In both cases the **C1P2** ligand binds six different An(IV) centers. This bonding is quite different from that seen with model complexes containing Ln^{3+} (Ln = lanthanide) cations where one of the **C1P2** oxygen atoms on each phosphonate moieties is protonated.[1a] The similarities between **NpC1P2−1** and **UC1P2−1** rapidly break down after this. Foremost among the differences is that the Np(IV) is eight-coordinate in **NpC1P2−1**, whereas the U(IV) in **UC1P2−1** is seven-coordinate. Therefore, at the most fundamental level the structural chemistry of Np(IV) is not being mimicked by U(IV).

The geometries of both of these high coordination number polyhedra found in **NpC1P2−1** and **UC1P2−1** deviate strongly from any idealized shape. In the case of **NpC1P2−1**, the Np(IV) centers are found as NpO_8 distorted dodecahedra with Np−O bond distances ranging from 2.216(3) to 2.648(3) Å. The two longest bonds of 2.595(3) and 2.648(3) Å are from the coordinating water molecules. These bond distances can be used to arrive at a bond-valence sum of 4.29 for Np(1), which is consistent with this compound containing Np(IV).[9] Sharply contrasting with **NpC1P2−1**, **UC1P2−1** contains UO_7 units that are not adequately described by common polyhedral designations such a capped octahedron or a capped trigonal prism. Instead they most closely resemble square antiprisms with a missing vertex. A UO_7 polyhedron containing U(IV) was previously recognized in U(UO_2)(PO_4)$_2$.[9] U−O bond distances are found to occur from 2.225(6) to 2.451(6) Å, where again the longest bond length of 2.451(6) Å is to the coordinating water molecule. The bond-valence sum for the U(1) atom is consistent with this compound containing U(IV), with a value of 4.18.[10] Selected bond distances for **NpC1P2−1** and **UC1P2−1** are given in Tables 2 and 3, respectively.

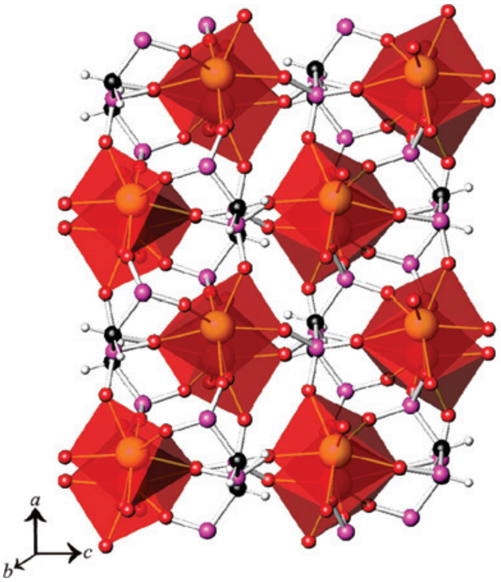

Figure 2. View down the *b* axis of the three-dimensional framework structure of U[$CH_2(PO_3)_2$](H_2O) (**UC1P2−1**). UO_7 units = red, oxygen = red, phosphorus = magenta, carbon = black, hydrogen = white.

Table 2. Selected Bond Distances (Å) for [Np($CH_2(PO_3)_2$](H_2O)$_2$ (**NpC1P2-1**)

	Distances (Å)		
Np(1)−O(3)	2.216(3)	P(1)−O(1)	1.519(3)
Np(1)−O(6)	2.253(3)	P(1)−O(3)	1.522(3)
Np(1)−O(5)	2.257(3)	P(1)−O(6)	1.524(3)
Np(1)−O(4)	2.263(3)	P(1)−C(1)	1.812(6)
Np(1)−O(2)	2.322(3)	P(2)−O(4)	1.506(3)
Np(1)−O(1)	2.385(3)	P(2)−O(5)	1.528(3)
Np(1)−O(8)	2.595(3)	P(2)−O(2)	1.534(4)
Np(1)−O(7)	2.648(3)	P(2)−C(1)	1.796(5)

Structure of (UO_2)$_2$[$CH_2(PO_3)_2$](H_2O)$_3$·H_2O (UC1P2−2). The structure of **UC1P2−2** is quite interesting in that it consists of UO_2^{2+} cations bound by **C1P2** to create both UO_6 tetragonal bipyramids and UO_7 pentagonal bipyramids. The

---

(7) Sheldrick, G. M. *SADABS 2001, Program for absorption correction using SMART CCD based on the method of Blessing*; Blessing, R. H. *Acta Crystallogr.* **1995**, *A51*, 33.

(8) Sheldrick, G. M. *SHELXTL PC, An Integrated System for Solving, Refining, and Displaying Crystal Structures from Diffraction Data*, Version 6.12; Siemens Analytical X-Ray Instruments, Inc.: Madison, WI, 2001.

(9) Benard, P.; Louer, D.; Dacheux, N.; Brandel, V.; Genet, M. *Chem. Mater.* **1994**, *6*, 1049.

(10) (a) Brese, N. E.; O'Keeffe, M. *Acta Crystallogr.* **1991**, *B47*, 192. (b) Brown, I. D. *The Chemical Bond in Inorganic Chemistry: The Bond Valence Model*; Oxford University Press: New York, 2002. (c) Brown, I. D.; Altermatt, D. *Acta Crystallogr.* **1985**, *B41*, 244.

Table 3. Selected Bond Distances (Å) for $U[CH_2(PO_3)_2](H_2O)$ **(UC1P2-1)**

Distances (Å)			
U(1)−O(5)	2.225(6)	P(1)−O(3)	1.515(6)
U(1)−O(1)	2.254(6)	P(1)−O(2)	1.524(7)
U(1)−O(6)	2.263(6)	P(1)−C(1)	1.803(9)
U(1)−O(3)	2.284(6)	P(2)−O(6)	1.523(6)
U(1)−O(2)	2.305(7)	P(2)−O(4)	1.525(6)
U(1)−O(4)	2.384(6)	P(2)−O(5)	1.526(6)
U(1)−O(7)	2.451(6)	P(2)−C(1)	1.795(8)
P(1)−O(1)	1.528(6)		

Table 4. Selected Bond Distances (Å) and Angles (°) for $(UO_2)_2[CH_2(PO_3)_2](H_2O)_3\cdot H_2O$ (**UC1P2-2**)

Distances (Å)			
U(1)−O(2)	1.759(4)	U(2)−O(13)	2.318(4)
U(1)−O(1)	1.788(5)	P(1)−O(7)	1.511(5)
U(1)−O(7)	2.276(4)	P(1)−O(12)	1.520(4)
U(1)−O(6)	2.328(4)	P(1)−O(13)	1.539(5)
U(1)−O(3)	2.426(5)	P(1)−C(1)	1.801(6)
U(1)−O(5)	2.426(5)	P(2)−O(6)	1.520(5)
U(1)−O(4)	2.464(5)	P(2)−O(11)	1.521(5)
U(2)−O(8)	1.782(4)	P(2)−O(10)	1.524(4)
U(2)−O(9)	1.783(4)	P(2)−C(1)	1.806(6)
U(2)−O(12)	2.256(4)		
U(2)−O(10)	2.269(4)		
U(2)−O(11)	2.289(4)		
Angles (°)			
O(2)−U(1)−O(1)	175.7(2)		

UO_6 units form the core of corrugated layers that extend in the [*bc*] plane and are terminated along the *a* direction by the UO_7 units, as shown in Figure 3. A particularly curious feature of the UO_7 units is that three of the five equatorial oxygen atoms are derived from coordinating water molecules. The water molecules point between the layers and form hydrogen bonding interactions with the interstitial water molecules. One way of looking at the layers is that the **C1P2** ligands first bridge between four uranyl centers that ultimately form the UO_6 tetragonal bipyramids. This leaves two remaining oxygen atoms on the methylenediphosphonate to chelate the second uranyl moiety. The remaining three sites in the UO_7 pentagonal bipyramid are the water molecules.

The UO_6 tetragonal bipyramids contain a uranyl core with two short U═O bond distances of 1.782(4) and 1.783(4) Å. The remaining four U—O bonds in the equatorial plane are normal, and range from 2.256(4) to 2.318(4) Å. The formal oxidation state for the U(2) center is +6 with a bond-valence sum of 6.13.[11] Likewise, the UO_7 polyhedra also contain a uranyl unit with U═O bond distances of 1.759(4) and 1.788(5) Å and equatorial distances ranging from 2.276(4) to 2.464(5) Å. These distances yield a bond-valence sum of 6.00.[11] Selected bond distances and angles are given in Table 4.

Structure of $UO_2[CH_2(PO_3H)_2](H_2O)$ (UC1P2−3). Single crystal X-ray diffraction data reveal a relatively straightforward three-dimensional network structure for **UC1P2−3**. There is, however, a twist to this structure in that it is polar. Both **NpC1P1−1** and **UC1P2−3** crystallize in the orthorhombic space group *Pna*2₁, which has a polar *c* axis. The origin of the polarity in **NpC1P1−1** is subtle; however, in **UC1P2−3** it is obvious. In $UO_2[CH_2$-

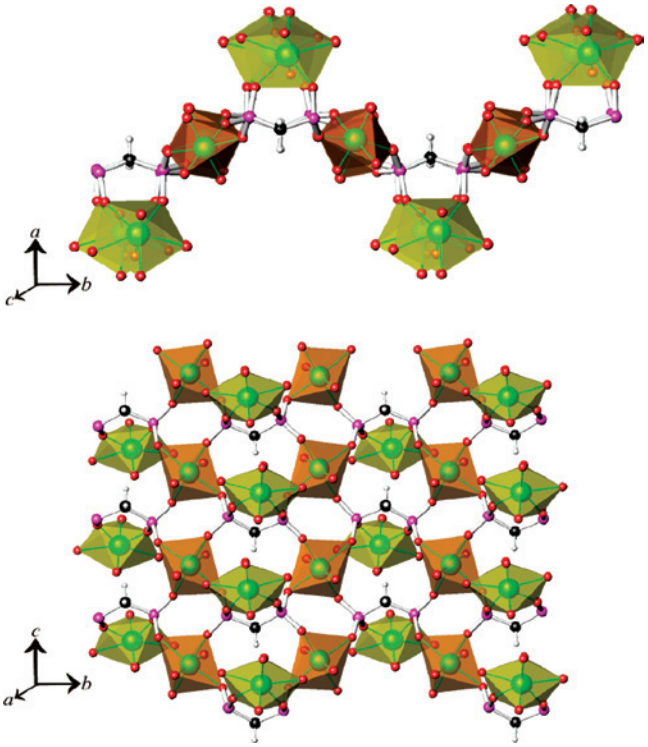

Figure 3. (Top) Depiction of part of the structure of $(UO_2)_2$-$[CH_2(PO_3)_2](H_2O)_3\cdot H_2O$ (**UC1P2−2**) showing the layers that extend in [*bc*] plane that consist of UO_6 and UO_7 units bound by methylenediphosphonate (**C1P2**). (Bottom) An illustration of the neutral layers in **UC1P2−2**. UO_6 tetragonal bipyramids = orange, UO_7 pentagonal bipyramids = yellow, oxygen = red, phosphorus = magenta, carbon = black, hydrogen = white.

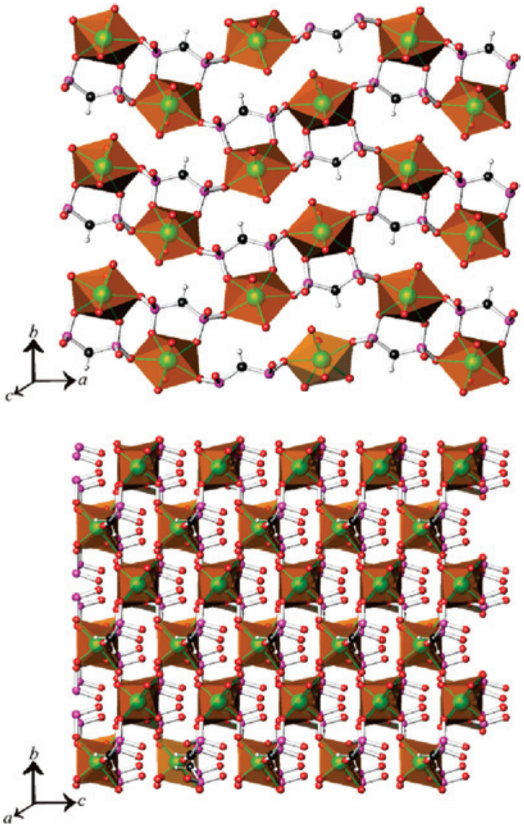

Figure 4. (Top) View down the *c* axis of the polar three-dimensional framework structure of $UO_2[CH_2(PO_3H)_2](H_2O)$ (**UC1P2−3**). (Bottom) A depiction of the structure of **UC1P2−3** showing the origin of the polarity where the protonated oxygen atoms on the methylenediphosphonate anions are oriented along the *c* axis.

Table 5. Selected Bond Distances (Å) and Angles (°) for $UO_2[CH_2(PO_3H)_2](H_2O)$ (**UC1P2-3**)

	Distances (Å)		
U(1)−O(4)	1.763(4)	P(1)−O(5)	1.520(3)
U(1)−O(6)	1.788(4)	P(1)−O(2)	1.577(3)
U(1)−O(1)	2.318(3)	P(1)−C(1)	1.796(5)
U(1)−O(3)	2.370(5)	P(2)−O(3)	1.502(4)
U(1)−O(5)	2.381(3)	P(2)−O(7)	1.520(3)
U(1)−O(7)	2.424(3)	P(2)−O(9)	1.577(6)
U(1)−O(8)	2.432(4)	P(2)−C(1)	1.780(5)
P(1)−O(1)	1.502(4)		
	Angles (°)		
O(4)−U1−O(6)	177.90(16)		

$(PO_3H)_2](H_2O)$, as the formula indicates, the **C1P2** ligand is diprotonated. The protonation of this ligand renders two of the oxygens atoms incapable of bonding with uranyl cations present in this structure. The location of protonation is obvious through comparisons of the length of the P−O bonds. The average P−O bond length for the oxygen atoms involved in coordinating the U(VI) cations is 1.511(4) Å, whereas the two terminal P−O bonds are 1.577(3) and 1.577(6) Å, indicating protonation at these sites. The P−OH groups are all oriented along the *c* axis, providing the origin of polarity in this structure. Two views of the structure of **UC1P2−3** are given in Figure 4.

Each **C1P2** ligand binds a total of three uranyl cations. One of these is through chelation, where each of the phosphonate moieties provides one oxygen atom for this interaction. The uranium centers are seven-coordinate, pentagonal bipyramids in this compound with two short U═O bonds defining the UO_2^{2+} cation. These distances are 1.763(4) and 1.788(4) Å. The five equatorial U−O bonds range from 2.318(3) to 2.432(4) Å. In total, these provide a bond-valence sum of 5.97.[11] There are no surprises in the oxidation states found in any of **C1P2** compounds. Selected bond distance and angles are given in Table 5.

Fluorescence Measurements on $(UO_2)_2[CH_2(PO_3)_2](H_2O)_3 \cdot H_2O$ (UC1P2−2) and $UO_2[CH_2(PO_3H)_2](H_2O)$ (UC1P2−3). The emission of green light that occurs from uranyl compounds when they are excited by long wavelength UV light has proven to be a useful diagnostic tool for a variety of purposes including energy transfer and detection.[12] One of the characteristic features of this emission is vibronic fine-structure, whose features have been assigned.[13] Fluorescence spectra for **UC1P2−2** and **UC1P2−3** were recorded from single crystals and are shown in Figure 5. These compounds show vibronic fine-structure typical for uranyl-containing compounds.[12,13] The features of **UC1P2−2** are somewhat broadened with respect to those of **UC1P2−3**.

Conclusions

In this work we have demonstrated that methylenediphosphonate can be used to link actinides in the +4 and +6 oxidation states into extended structures that some might term coordination polymers or metal-organic frameworks. Three of the four compounds possess three-dimensional networks and one is layered. The structural chemistry of actinide diphosphonates is extremely rich because when a polydentate ligand like methylenediphosphonate is combined with the high-coordination numbers and structural flexibility of the actinides many bonding possibilities result.

The ionic radii of 8-fold coordinated U(IV) and Np(IV) are quite similar at 1.00 Å and 0.98 Å, respectively.[14] Both cations are most commonly found in solids in eight- and nine-coordinate environments.[15] There are numerous examples of isostructural U(IV) and Np(IV) compounds.[15] Nevertheless, there is an ongoing debate about whether early actinides like ^{232}Th(IV) and ^{238}U(IV), or even nonradioactive Ce(IV) and Zr(IV), can be used as surrogates for more potentially hazardous transuranium elements like ^{237}Np(IV)

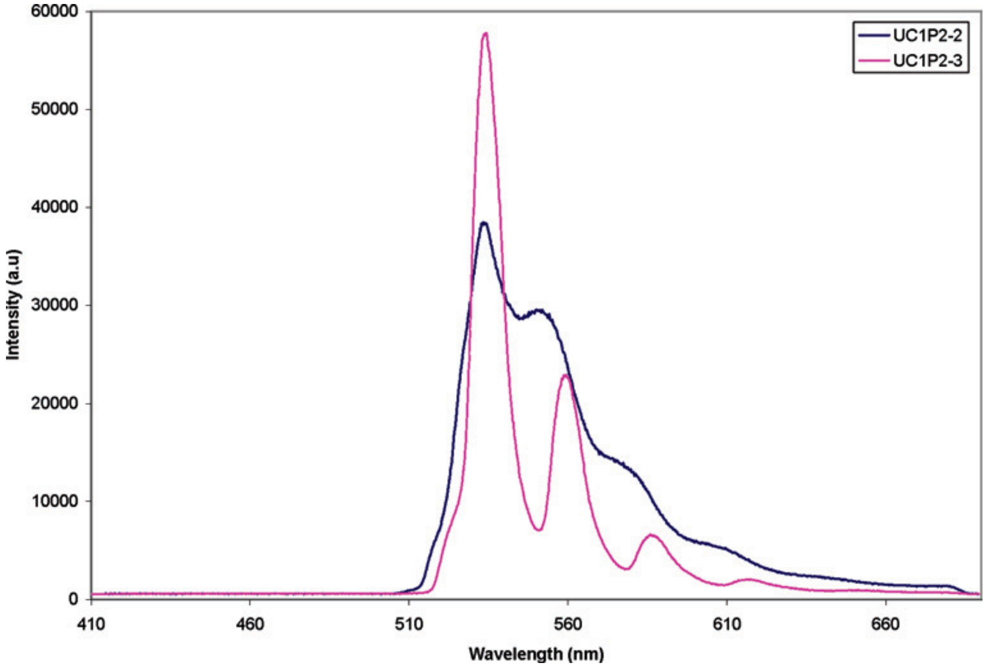

Figure 5. Fluorescence spectra of $(UO_2)_2[CH_2(PO_3)_2](H_2O)_3 \cdot H_2O$ (**UC1P2−2**) and $UO_2[CH_2(PO_3H)_2](H_2O)$ (**UC1P2−3**) showing vibronic fine-structure typical for uranyl-containing compounds.

and ^{239}Pu(IV).[6] The fact is that while **NpC1P2−1** and **UC1P2−1** were both produced under similar conditions, they do possess different structures and compositions. Thus, here we find another instance where it is clear that if one is going to understand the crystal chemistry of a transuranium element, one must actually work with the element in question and not a surrogate.[16] This is contrary to that often observed for U(IV) and Np(IV) phosphate compounds that are heated to higher temperatures.[6,17–20] To further illustrate potential differences, we point to the $Th_4(PO_4)_4P_2O_7$ structure type, which is under consideration as a possible host material for the long-term storage of transuranium elements.[16] It has been shown that this phase can incorporate U(IV) and Pu(IV) but not the surrogates Ce(IV) or Zr(IV).[16] The former is reduced to Ce(III), and the latter is too small to stabilize this lattice.[16] Furthermore, while $M_2O(PO_4)_2$ phases can be prepared when M = Zr, Th, U, and Np, attempts to prepare the Ce(IV) and Pu(IV) analogs result in spontaneous reduction to Ce(III) and Pu(III), and monazite-like phases with the composition MPO_4 result.[20]

Another observation of particular interest is the demonstration that the in situ hydrothermal reduction of Np(VI) to Np(IV) is not unique to the methylphosphonate system[5] but rather is a more general reaction. In fact, our observations are thus far that this reaction is normal under the hydrothermal conditions described and can only be prevented by the incorporation of an oxidant.[5] This reduction chemistry also occurs with U(VI), albeit to a very small extent.

Acknowledgment. This work was supported by the Chemical Sciences, Geosciences and Biosciences Division, Office of Basic Energy Sciences, Office of Science, Heavy Elements Program, U.S. Department of Energy under Grant DE-FG02-01ER15187, and by the Malone-Zallen Graduate Research Fund (to T.H.B.), and a Harry Merriwether Fellowship (to T.H.B.).

Supporting Information Available: X-ray crystallographic files in CIF format for $Np[CH_2(PO_3)_2](H_2O)_2$ (**NpC1P2−1**), $U[CH_2(PO_3)_2](H_2O)$ **(UC1P2−1)** $(UO_2)_2[CH_2(PO_3)_2](H_2O)_3\cdot H_2O$ (**UC1P2−2**), and $UO_2[CH_2(PO_3H)_2](H_2O)$ (**UC1P2−3**). This material is available free of charge via the Internet at http://pubs.acs.org.

IC800255H

---

(11) Burns, P. C.; Ewing, R. C.; Hawthorne, F. C. *Can. Mineral.* **1997**, *35*, 1551.

(12) (a) Grohol, D.; Clearfield, A. *J. Am. Chem. Soc.* **1997**, *119*, 4662. (b) Almond, P. M.; Talley, C. E.; Bean, A. C.; Peper, S. M.; Albrecht-Schmitt, T. E. *J. Solid State Chem.* **2000**, *154*, 635. (c) Yu, Y.; Zhan, W.; Albrecht-Schmitt, T E. *Inorg. Chem.* **2007**, *46*, 10214. (d) Frisch, M.; Cahill, C. L. *Dalton Trans.* **2006**, *39*, 4679. (e) Cahill, C. L.; de Lill, D. T.; Frisch, M. *CrystEngComm* **2007**, *9*, 15.

(13) Denning, R. G.; Norris, J. O. W.; Short, I. G.; Snellgrove, T. R.; Woodwark, D. R. In *Lanthanide and Actinide Chemistry and Spectroscopy*; Edelstein, N. M., Ed.; ACS Symposium Series 131; American Chemical Society: Washington, DC, 1980; Chapter 15.

(14) Shannon, R. D. *Acta Crystallogr.* **1976**, *A32*, 751.

(15) (a) Penneman, R. A.; Ryan, R. R.; Rosenzweig, A. *Struct. Bonding (Berlin)* **1973**, *13*, 1. (b) Brandel, V.; Dacheux, N. *J. Solid State Chem.* **2004**, *177*, 4755. (c) Brandel, V.; Dacheux, N. *J. Solid State Chem.* **2004**, *177*, 4743.

(16) Dacheux, N.; Podor, R.; Brandel, V.; Genet, M. *J. Nucl. Mater.* **1998**, *252*, 179.

(17) Dacheux, N.; Grandjean, S.; Rousselle, J.; Clavier, N. *Inorg. Chem.* **2007**, *46*, 10390.

(18) Dacheux, N.; Thomas, A. C.; Brandel, V.; Genet, M. *J. Nucl. Mater.* **1998**, *257*, 108.

(19) Keller, C.; Walter, K. H. *J. Inorg. Nucl. Chem.* **1965**, *27*, 1253.

(20) Dacheux, N.; Clavier, N.; Wallez, G.; Quarton, M. *Solid State Sci.* **2007**, *9*, 619.